Sensitivity analysis of voltage-gated ion channel models.

Alon Korngreen[1,2]

1. The Leslie and Susan Gonda Interdisciplinary Brain Research Center, Bar Ilan University, Ramat Gan 5290002, Israel

2. The Mina and Everard Goodman Faculty of Life Sciences, Bar Ilan University, Ramat Gan 5290002, Israel

Abbreviated title: parameter sensitivity in ion channel models

Keywords: Parameter sensitivity, model, Markov chain, voltage-gated ion channels

Corresponding author:
Prof. Alon Korngreen, Bar Ilan University,
The Leslie and Susan Gonda Interdisciplinary Brain Research Center,
The Mina and Everard Goodman Faculty of Life Sciences,
Ramat Gan 5290002, Israel
E-mail: alon.korngreen@biu.ac.il

Abstract

Modeling voltage-gated ion channel function is essential for understanding neuronal excitability. However, finding the right balance between model complexity and practicality is a significant challenge. In this study, I explored how sensitive Markov models of ion channels were to different parameters, beginning with a straightforward two-state system and progressing to more intricate three- and four-state models. Through tests using step voltage and sine wave protocols, I discovered clear sensitivity patterns during both the activation and deactivation phases. As expected, forward transitions were most influential during activation, while reverse transitions became more pronounced during deactivation. Notably, I found that transitions between closed states had minimal impact on the overall whole-cell current or the opening probability (P_o). This underscores a significant limitation in relying on these measurements to constrain specific parameters. These results highlight the strengths and limitations of Markov models, showing that their effectiveness can be restricted by how sensitive parameters are to the protocols used in experiments. My findings set clear guidelines on the level of complexity feasible in Markov models of voltage-gated ion channels and offer insights that can help create more efficient and reliable models of neuronal excitability.

Introduction

Understanding how the brain computes is one of the most profound challenges facing humanity in the 21st century (Crick, 1989; Crick and Koch, 2003; Yuste and Church, 2014). Neurons, the fundamental units of the brain, are responsible for processing and transmitting information through electrical and chemical signals. However, despite decades of research, the precise nature of the computations performed by individual neurons remains an area of active investigation (Hausser et al., 2000; Spruston and Kath, 2004; Silver, 2010; Stuart and Spruston, 2015). The conventional view of neurons as simple integrators of inputs, firing action potentials in response to the summation of excitatory and inhibitory signals, has been challenged by findings demonstrating that neurons perform far more complex computations (Segev and Rall, 1998; Segev and Schneidman, 1999; Koch and Segev, 2000; London and Segev, 2001; Poirazi and Mel, 2001; Poirazi et al., 2003; Stuart and Spruston, 2015). This realization is reshaping the field of computational neuroscience, driving researchers to develop more sophisticated models that capture the intricate behavior of individual neurons (Rapp et al., 1996; Roth and Häusser, 2001; Wood et al., 2004; Druckmann et al., 2007; Hines et al., 2008; Toledo-Rodriguez et al., 2008; Hay et al., 2011; Hendrickson et al., 2011; Schoen et al., 2012).

One of the primary approaches to unraveling neurons' computational properties is the development of mathematical and computational models (Rall, 1962, 1964, 1969; Segev and Rall, 1998; Hines et al., 2008; King et al., 2009; Markram et al., 2015). In computational neuroscience, models range from highly abstract representations that simplify neurons as point-like integrators to biologically detailed simulations incorporating the full complexity of a neuron's structure and biophysics (Segev and Schneidman, 1999; Carnevale and Hines, 2006; Hay et al., 2013; Markram et al., 2015). The latter, often called "realistic" models, have become increasingly feasible thanks to advances in experimental techniques and computational resources. These models attempt to recreate neurons' complete electrical and chemical environment, allowing researchers to simulate how neurons process information under various conditions. By incorporating detailed data on ion channel kinetics and distributions, dendritic branching patterns, and synaptic input dynamics, realistic models provide a powerful tool for exploring the computations performed by individual neurons.

Key elements allowing experimental reduction of parameter space are voltage-gated ion channels. Voltage-gated ion channels are responsible for most non-linear responses in the nervous system and are a significant component of biologically detailed models (Koch, 1998; Koch and Segev, 2000; Roux et al., 2004). Since the days of Hodgkin and Huxley, numerous studies have recorded ionic currents from voltage-gated channels and reduced these currents to a set of differential equations to explain neuronal physiology. Developing a family of modern ion channel models that are computationally efficient, robust, and can accurately reproduce neuronal physiology is important. To achieve this, it is essential to trust the models of ion channels used. To generate physiologically relevant models of ion channels, a pipeline should be devised that enables the systematic and reliable generation of such models. How can we generate robust models for voltage-gated ion channels? I investigated this question using global parameter sensitivity methods (Saltelli et al., 2008). I demonstrate that standard Markov models are insensitive to specific parameters that define the model. The analysis I present here limits the complexity of Markov models for voltage-gated ion channels and can be used to design robust building blocks for biologically detailed models of neuronal excitability.

Methods

Markov models of voltage-gated ion channels

In a standard Markov model for an ion channel with N states, the rate constants are represented by a conventional N×N rate matrix, denoted as Q (Sakmann and Neher, 1995). In this matrix, each off-diagonal element represents the rate constant for the transition from state i to state j. Each diagonal element equals the negative sum of the off-diagonal elements in that row, ensuring that each row's total is zero. If there is no direct transition from state i to state j, the corresponding element k_{ij} is set to zero. For voltage-gated channels, the simplest definition of the forward rate constant k_{ij} comprises a pre-exponential factor A_{ij}. Additionally, an exponential factor, denoted as z_{ij}, is multiplied by the magnitude of the membrane potential, V. More complex functional representations for the voltage dependence of the rate constant (Destexhe, 2000; Destexhe and Huguenard, 2000). In this study, I used only this simple one.

Eqn 1.

$$k_{ij} = A_{ij} e^{-V/z_{ij}}$$

For forward rate constants, z_{ij} is negative, and for backward rate constants, z_{ij} is positive. This exponential factor can also depend on factors such as charge, pressure, temperature, and others (Hille, 1992). At any given moment, a state probability vector P, which has a dimension of N, represents the occupancy of the N states in the model. The Kolmogorov differential equation describes the dynamics of a Markov process (Sigg, 2014).

Sensitivity analysis

Sensitivity analysis evaluates how uncertain parameters influence the variability of model outputs. Numerous sensitivity measures are available (Hamby, 1994; Saltelli et al., 2008; Zi, 2011). In this study, I employed a global variance-based sensitivity analysis that calculates Sobol sensitivity indices, a well-established approach (Sobol, 2001). This global and non-intrusive method allows us to investigate interactions among model parameters (Zi, 2011). Interactions occur when the combined effects of parameters on the output are non-additive.

Eqn. 2

$$S_i = \frac{V[E[Y|Q_i]]}{V[Y]}$$

Several Sobol' indices exist, with the first-order Sobol sensitivity index (S_i) being the most commonly used. S_i measures the direct influence of each parameter on the model output variance. $E[Y|Q_i]$ represents the expected value of the output Y when the parameter Q_i is held constant. $V\left[E[Y|Q_i]\right]$ quantifies the variance explained by Q_i alone, and V[Y] is the variance of the output. The first-order Sobol sensitivity index indicates how much the model's variance is expected to decrease when parameter Q_i is held constant. For example, if S_i =0.3, then 30% of the output variance is explained by Q_i alone. The sum of all first-order Sobol sensitivity indices cannot exceed one and will only equal one if there are no interactions between parameters (Glen and Isaacs, 2012).

In this study, I also calculated the total sensitivity indices.

Eqn. 3

$$S_{Ti} = \frac{V[E[Y|Q_{-i}]]}{V[Y]}$$

$E[Y|Q_{-i}]$ represents the expected value of the output Y when all parameters, except Q_i, are held constant. $V\left[E[Y|Q_{-i}]\right]$ quantifies the variance explained by all variables except Q_i. For example, if S_{Ti} =0.5, then Q_i (including its interactions with other variables) explains 50% of the output variance.

All simulations were carried out using custom Python code and the SALib sensitivity analysis library (Herman and Usher, 2017). The code is available in a GitHub repository at https://github.com/alon67/MarkovSensitivity and will be made public upon publication.

Results

The simplest Markov model for an ion channel consists of two states: a closed state and an open state (Scheme 1). For a voltage-gated channel, the rate constants that describe the transitions between these states are voltage-dependent, as detailed in the Methods section. This straightforward model includes four free parameters. To assess the model's sensitivity to variations in these parameters, I established the range for A_{12} and A_{21} as 0.0001 to 1 msec-1, while z_{12} and z_{21} are defined within a range of 1 to 80 mV. This range aligns with the physiological limits for these parameters. Figure 1A presents 500 simulations of the channel's opening probability (P_o) in response to a voltage step from -80 mV to +10 mV. The simulations were performed with randomly selected parameters within the prescribed range. The average response across 32,000 simulations is depicted in red. As anticipated, the sensitivity index for most of the model's parameters, except for A_{21}, remained low at the holding potential of -80 mV (Figs 1B and 1C). The elevated sensitivity index for A_{21} suggests a high probability that the model will be in the closed state at this membrane potential. Following the voltage step to +10 mV, the sensitivity index of A_{12} increased, while that for A_{21} decreased, reflecting the rise in P_o. The transient changes to the sensitivity index of z_{12} and z_{21} highlight the model's relaxation following activation and deactivation, respectively.

$$C \underset{k_{21}=A_{21}\exp(V/z_{21})}{\overset{k_{12}=A_{12}\exp(-V/z_{12})}{\rightleftharpoons}} O$$

Scheme 1

One specific condition reduces the model from a four-parameter model to a two-parameter model. A voltage step to zero millivolt nulls the exponential part of the rate constants. Thus, it was possible to predict that the sensitivity index for z_{12} and z_{21} would be zero at this potential. In other words, the model will be insensitive to changes to these parameters. I performed this simulation as a sanity check of the Python code I wrote for this project. Indeed, stepping from -80 mV to 0 mV caused a decrease in the S_i values of z_{12} and z_{21} to zero (Fig. 2).

It has been suggested that a fast-changing large-amplitude voltage command may be more suitable for probing ion channel kinetics (Millonas and Hanck, 1998; Kargol et al., 2002, 2004; Beattie et al., 2018). To test whether a rapidly oscillating voltage protocol would produce better parameter sensitivity, I simulated the model's response to a 100 Hz sine

wave. The amplitude of this stimulus ranged from -80 to +80 mV. Representative simulations are shown in Fig. 3A as thin lines, and a thick red line represents the population average. The sensitivity indices followed a similar pattern to that I obtained when the model was stimulated using a step voltage. The sensitivity of the model to A_{12} increased during channel activation (Fig. 3B). In contrast, its sensitivity to A_{21} increased during deactivation (Fig. 3C). The parameters related to the voltage dependence of the channel (z_{12} & z_{21}) displayed transient sensitivity similar to that observed in Figure 1. Thus, the oscillating voltage protocol triggered a parameter sensitivity similar to that of the standard one.

The two-state Markov model can be used to reproduce only a small part of the ion channel kinetics observed in nature. Most Markov models of ion channel kinetics contain longer chains of states. To extend the current discussion to more complex Markov models, I simulated parameter sensitivity for a three-state model.

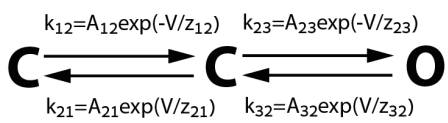

Scheme 2

The results of this simulation, applying a step voltage from -80 mV to 10 mV, are shown in Figure 4. The opening probability of the model was sensitive to changes in the parameters that define the two forward transitions (Figs 4A & 4C). The model was also sensitive to the parameters of the backward transition from the open state to the second closed state (Fig. 4D). As expected ,this transition was mainly sensitive during channel deactivation. Interestingly, the model showed almost no sensitivity to the parameters of the backward transition between the first and second closed states (Fig. 4B). The total sensitivity indices (S_{Ti}) followed a similar pattern with the two forward transitions (Fig. 4E & 4G) and the backward transition from the open state to the first closed state (Fig. 4H) contributing to the overall variance of the model. However, the parameters defining the backward transition from the first to the second closed state contributed little to the total variance (Fig. 4F). Using a 100 Hz sine voltage command produced a similar parameter sensitivity pattern, where all parameters except those defining the transitions between closed states influenced the variance of the model's output (Fig. 5). I performed simulations similar to those presented in Figures 4 & 5 also on a linear Markov model with three closed states. These simulations were not included in the manuscript, but they reproduced similar results, in which

parameters defining backward rate constants, which were not connected to the open state, contributed little to the variance of the model's output.

Discussion

In this study, I examined parameter sensitivity of Markov models that describe voltage-gated ion channel kinetics, focusing on balancing model complexity and interpretability. By applying global sensitivity analysis to two- and three-state models, I identified consistent patterns in how different parameters influence model behavior under various stimulation protocols. A key finding across all tested models was the low sensitivity of backward transitions between closed states, especially those not directly connected to the open state. These transitions contributed little to the channel's opening probability, making it difficult to constrain them with whole-cell recordings alone. My findings provide clear guidelines on the level of complexity feasible in Markov models of voltage-gated ion channels, offering insights that can help develop more efficient and reliable models of neuronal excitability.

Under standard step voltage protocols, forward transition rates were most influential during activation (Figs. 1-5), whereas reverse transition rates dominated during deactivation. This aligns with the expected biophysical behavior of voltage-gated channels, where state transitions closely follow changes in membrane potential and opening probability (P_o). Voltage-dependent parameters (z_{12}, z_{21}) showed transient sensitivity during both activation and deactivation, underscoring their role in fine-tuning gating transitions. To test whether dynamic voltage commands could better probe model parameters, I applied a 100 Hz sine wave stimulus (Figs 3 & 5). While this oscillatory protocol modestly increased sensitivity to some reverse transitions, the overall pattern remained unchanged: transitions between closed states contributed little to the variance of the model's output. Thus, although non-stationary stimuli can refine specific parameter estimates, they cannot fully overcome the inherent limitations of using P_o or whole-cell currents as the sole optimization targets. A critical condition, nullifying exponential rate constants at zero mV, served as a validation check for our simulations. As predicted, sensitivity indices for voltage-dependent parameters (z12, z21) dropped to zero under this condition, confirming the robustness of the computational framework. This result underscores the importance of sanity checks in computational modeling, particularly when integrating stochastic optimization algorithms that necessitate extensive parameter exploration (Keren et al., 2005; Gurkiewicz and Korngreen, 2007; Menon et al., 2009; Hay et al., 2011; Ben-Shalom et al., 2012).

The Hodgkin–Huxley formalism, which can be seen as a variant of the simplest Markov scheme, inherently avoids many of these issues because all gating variables describe transitions directly linked to the open state and gating is a concerted mechanism (Hodgkin and Huxley, 1952). In contrast, extended Markov chains with long closed- or inactivated-state sequences introduce parameters that are effectively invisible to macroscopic recordings. This not only complicates optimization but also risks overfitting without improving predictive accuracy.

The implications of these results are twofold. First, they highlight the limitations of standard experimental protocols and data types in optimizing complex Markov models. While whole-cell current measurements provide essential insights, they cannot capture state transitions that do not affect channel opening. This limitation poses challenges for stochastic optimization methods, such as genetic algorithms or simulated annealing, as low-sensitivity parameters exert minimal influence on cost functions, hindering their convergence.

Second, our results provide practical guidelines for reducing model complexity. Given the insensitivity of certain parameters, simplified Markov models that exclude poorly constrained transitions can achieve similar accuracy with reduced computational costs. This approach is particularly relevant for biologically detailed neuronal models, where parameter inflation can compromise model interpretability and efficiency. It may appear that avoiding long chains of closed states poses too significant a restriction on voltage-gated ion channel models. However, as suggested in Figure 6, several schemes, particularly those utilizing circular transitions, can be employed to generate complex models. The use of circular transitions reduces some complexity as it takes microscopic reversibility into account (Colquhoun et al., 2004). It is interesting to note that a study applying a topology-mutating genetic algorithm for optimizing the best state diagram and transition-rate parameters of a voltage-gated ion channel model generated transition diagrams that did not contain long closed state chains (Menon et al., 2009).

Ion channels play a pivotal role in neuronal excitability, and advancements in patch-clamp techniques have significantly improved our understanding of their behavior. However, bridging the gap between experimental data and computational models remains a major challenge(Nowotny and Selverston, 2007; Road, 2009; Almog and Korngreen, 2014, 2016; Lampert and Korngreen, 2014; Daly et al., 2015; Almog et al., 2022). The Hodgkin-Huxley framework, while widely used, differs fundamentally from Markov models preferred by

biophysicists for their mechanistic detail. Optimizing Markov models requires protocols and cost functions that are sensitive to all relevant parameters, a condition not always met with existing experimental paradigms.

In conclusion, this study demonstrates that parameter sensitivity in Markov models of ion channels is highly protocol-dependent, with activation and deactivation exhibiting distinct sensitivity patterns. Oscillating protocols, while beneficial, remain limited in their ability to constrain parameters describing deep closed-closed transitions. These findings establish practical constraints on model complexity and underscore the need for targeted experimental strategies to enhance parameter identifiability. Future work should explore hybrid approaches that combine macroscopic current measurements with single-channel data to achieve a more comprehensive understanding of ion channel kinetics.

Figure Legends

Figure 1: Sensitivity analysis of a two-state Markov model of a voltage-gated ion channel. A, representative simulation traces (gray lines) and population average (red line) of changes to the model's opening probability (P_o) in response to a voltage step from -80 mV to +10 mV. B, sensitivity indices (S_i) for the transition from the closed state to the open state in Scheme 1 plotted over time. C, same as in B, for the transition from the open state to the closed state.

Figure 2: Sanity check of the sensitivity analysis for a two-state Markov model. A, changes in the sensitivity indices (S_i) for the transition from the closed state to the open state in Scheme 1 in response to a voltage step from -80 mV to 0 mV, plotted over time. B, same as in A, for the transition from the open state to the closed state.

Figure 3: Sensitivity analysis of a two-state Markov model's response to non-stationary stimulation. A, representative simulation traces (gray lines) and the population average (red line) of changes in the model's opening probability (P_o) in response to a sinusoidal voltage command at 100 Hz. B, sensitivity indices (S_i) for the transition from the closed state to the open state in Scheme 1 plotted over time. C, same as in B, for the transition from the open state to the closed state.

Figure 4: Sensitivity analysis of a three-state Markov model of a voltage-gated ion channel. A, B, C, and D show the changes in sensitivity indices (S_i) for the model in Scheme 2 in response to a voltage step from -80 mV to 0 mV, plotted over time. E, F, G, and H display the total sensitivity indices (S_{Ti}) for the same model, also in response to the voltage step from -80 mV to 0 mV, plotted over time.

Figure 5: Sensitivity analysis of a three-state Markov model's response to non-stationary stimulation. A, B, C, and D show changes in the sensitivity indices (S_i) for the model displayed in Scheme 2 in response to a sinusoidal voltage command at 100 Hz, plotted over time. E, F, G, and H show total sensitivity indices (S_{Ti}) for the same model and stimulus, also plotted over time.

Figure 6: Markov model schemes in which all states are only one transition away from the open state.

References

Almog, M., Degani-Katzav, N., and Korngreen, A. (2022). Kinetic and thermodynamic modeling of a voltage-gated sodium channel. *European Biophysics Journal* 51. doi: 10.1007/s00249-022-01591-3

Almog, M., and Korngreen, A. (2014). A quantitative description of dendritic conductances and its application to dendritic excitation in layer 5 pyramidal neurons. *The Journal of Neuroscience* 34, 182–96. doi: 10.1523/JNEUROSCI.2896-13.2014

Almog, M., and Korngreen, A. (2016). Is realistic neuronal modeling realistic? *J Neurophysiol* 116. doi: 10.1152/jn.00360.2016

Beattie, K. A., Hill, A. P., Bardenet, R., Cui, Y., Vandenberg, J. I., Gavaghan, D. J., et al. (2018). Sinusoidal voltage protocols for rapid characterisation of ion channel kinetics. *Journal of Physiology* 596. doi: 10.1113/JP275733

Ben-Shalom, R., Aviv, A., Razon, B., and Korngreen, A. (2012). Optimizing ion channel models using a parallel genetic algorithm on graphical processors. *Journal of neuroscience* 206, 189–194. doi: 10.1016/j.jneumeth.2012.02.024

Carnevale, N. T., and Hines, M. L. (2006). *The NEURON book*. Cambridge, UK ; New York: Cambridge University Press.

Colquhoun, D., Dowsland, K., Beato, M., and Plested, A. (2004). How to impose microscopic reversibility in complex reaction mechanisms. *Biophys J* 86, 3510–3518. doi: 10.1529/biophysj.103.038679

Crick, F. (1989). The recent excitement about neural networks. *Nature* 337. doi: 10.1038/337129a0

Crick, F., and Koch, C. (2003). A framework for consciousness. *Nat Neurosci* 6, 119–126. Available at: http://www.ncbi.nlm.nih.gov/entrez/query.fcgi?cmd=Retrieve&db=PubMed&dopt=Citation&list_uids=12555104

Daly, A. C., Gavaghan, D. J., Holmes, C., and Cooper, J. (2015). Hodgkin–Huxley revisited: Reparametrization and identifiability analysis of the classic action potential model with approximate Bayesian methods. *R Soc Open Sci* 2. doi: 10.1098/rsos.150499

Destexhe, A. (2000). "kinetic models of membrane excitability and synaptic interactions," in *computational models of molecular and cellular interactions*, eds. J. Bower and H. Bolouri (Cambridge, USA: MIT Press), 225–262.

Destexhe, A., and Huguenard, J. (2000). "Which formalism to use for modeling voltage-dependent conductances?," in *Computational Neuroscience: Realistic Modeling for Experimentalists*, ed. E. DeSchutter (Boca Raton, FL: CRC Press), 129–157. Available at: http://cns.iaf.cnrs-gif.fr/abstracts/desh99.html

Druckmann, S., Banitt, Y., Gidon, A., Schürmann, F., Markram, H., and Segev, I. (2007). A novel multiple objective optimization framework for constraining conductance-based neuron models by experimental data. *Front Neurosci* 1. Available at: http://www.ncbi.nlm.nih.gov/pmc/articles/PMC2570085/ (Accessed June 23, 2014).

Glen, G., and Isaacs, K. (2012). Estimating Sobol sensitivity indices using correlations. *Environmental Modelling and Software* 37. doi: 10.1016/j.envsoft.2012.03.014

Gurkiewicz, M., and Korngreen, A. (2007). A numerical approach to ion channel modelling using whole-cell voltage-clamp recordings and a genetic algorithm. *PLoS Comput Biol* 3, e169. doi: 10.1371/journal.pcbi.0030169

Hamby, D. M. (1994). A review of techniques for parameter sensitivity analysis of environmental models. *Environ Monit Assess* 32. doi: 10.1007/BF00547132

Hausser, M., Spruston, N., and Stuart, G. J. (2000). Diversity and dynamics of dendritic signaling. *Science (1979)* 290, 739–744. doi: 8934 [pii]

Hay, E., Hill, S., Schürmann, F., Markram, H., and Segev, I. (2011). Models of neocortical layer 5b pyramidal cells capturing a wide range of dendritic and perisomatic active properties. *PLoS Comput Biol* 7, e1002107. doi: 10.1371/journal.pcbi.1002107

Hay, E., Schürmann, F., Markram, H., and Segev, I. (2013). Preserving axosomatic spiking features despite diverse dendritic morphology. *J Neurophysiol* 109, 2972–81. doi: 10.1152/jn.00048.2013

Hendrickson, E. B., Edgerton, J. R., and Jaeger, D. (2011). The capabilities and limitations of conductance-based compartmental neuron models with reduced branched or unbranched morphologies and active dendrites. *J Comput Neurosci* 30, 301–321. doi: 10.1007/s10827-010-0258-z

Herman, J., and Usher, W. (2017). SALib: An open-source Python library for Sensitivity Analysis. *The Journal of Open Source Software* 2. doi: 10.21105/joss.00097

Hille, B. (1992). *Ionic channels of excitable membranes*., 2nd Edn. Sunderland, Mass.: Sinauer Associates.

Hines, M. L., Markram, H., and Schürmann, F. (2008). Fully implicit parallel simulation of single neurons. *J Comput Neurosci* 25, 439–448. doi: 10.1007/s10827-008-0087-5

Hodgkin, A. L., and Huxley, A. F. (1952). A quantitative description of membrane current and its application to conduction and excitation in nerve. *J Physiol* 117, 500–544. Available at: http://www.ncbi.nlm.nih.gov/entrez/query.fcgi?cmd=Retrieve&db=PubMed&dopt=Citation&list_uids=12991237 (Accessed July 2, 2014).

Kargol, A., Hosein-Sooklal, A., Constantin, L., and Przestalski, M. (2004). Application of oscillating potentials to the Shaker potassium channel. *Gen Physiol Biophys* 23.

Kargol, A., Smith, B., and Millonas, M. M. (2002). Applications of nonequilibrium response spectroscopy to the study of channel gating. Experimental design and optimization. *J Theor Biol* 218. doi: 10.1006/jtbi.2002.3073

Keren, N., Peled, N., and Korngreen, A. (2005). Constraining compartmental models using multiple voltage recordings and genetic algorithms. *J Neurophysiol* 94, 3730–3742. doi: 10.1152/jn.00408.2005

King, J. G., Hines, M., Hill, S., Goodman, P. H., Markram, H., and Schürmann, F. (2009). A component-based extension framework for large-scale parallel simulations in NEURON. 3, 1–11. doi: 10.3389/neuro.11.010.2009

Koch, C. (1998). *Biophysics of Computation*. Oxford,UK: Oxford University Press. doi: 10.1093/oso/9780195104912.001.0001

Koch, C., and Segev, I. (2000). The role of single neurons in information processing. *Nat Neurosci* 3 Suppl, 1171–1177. Available at:

http://www.ncbi.nlm.nih.gov/entrez/query.fcgi?cmd=Retrieve&db=PubMed&dopt=Citation&list_uids=11127834

Lampert, A., and Korngreen, A. (2014). *Markov Modeling of Ion Channels : Implications for Understanding Disease*., 1st Edn. Elsevier Inc. doi: 10.1016/B978-0-12-397897-4.00009-7

London, M., and Segev, I. (2001). Synaptic scaling in vitro and in vivo. *Nat Neurosci* 4, 853–855. Available at: http://www.ncbi.nlm.nih.gov/entrez/query.fcgi?cmd=Retrieve&db=PubMed&dopt=Citation&list_uids=11528406

Markram, H., Muller, E., Ramaswamy, S., Reimann, M. W., Abdellah, M., Sanchez, C. A., et al. (2015). Reconstruction and Simulation of Neocortical Microcircuitry. *Cell* 163, 456–492. doi: 10.1016/j.cell.2015.09.029

Menon, V., Spruston, N., and Kath, W. L. (2009). A state-mutating genetic algorithm to design ion-channel models. *Proceedings of the National Academy of Science* 106, 16829–16834.

Millonas, M. M., and Hanck, D. A. (1998). Nonequilibrium response spectroscopy of voltage-sensitive ion channel gating. *Biophys J* 74, 210–229. Available at: http://www.ncbi.nlm.nih.gov/entrez/query.fcgi?cmd=Retrieve&db=PubMed&dopt=Citation&list_uids=9449324

Nowotny, T., and Selverston, A. I. (2007). Models Wagging the Dog : Are Circuits Constructed with Disparate Parameters ? 2003, 1985–2003.

Poirazi, P., Brannon, T., Mel, B. W., and Heraklion, G. R. (2003). Pyramidal Neuron as Two-Layer Neural Network. 37, 989–999.

Poirazi, P., and Mel, B. W. (2001). Impact of active dendrites and structural plasticity on the memory capacity of neural tissue. *Neuron* 29, 779–796. doi: S0896-6273(01)00252-5 [pii]

Rall, W. (1962). Electrophysiology of a dendritic neuron model. *Biophys J* 2, 145–167. Available at: http://www.ncbi.nlm.nih.gov/entrez/query.fcgi?cmd=Retrieve&db=PubMed&dopt=Citation&list_uids=14490040

Rall, W. (1964). Theoretical Significance of Dendritic Trees for Neuronal Input-Output Relations. *Neural theory and modeling*.

Rall, W. (1969). Distributions of potential in cylindrical coordinates and time constants for a membrane cylinder. *Biophys J* 9, 1509–41. doi: 10.1016/S0006-3495(69)86468-4

Rapp, M., Yarom, Y., and Segev, I. (1996). Modeling back propagating action potential in weakly excitable dendrites of neocortical pyramidal cells. *Proc Natl Acad Sci U S A* 93, 11985–11990. Available at: http://www.ncbi.nlm.nih.gov/entrez/query.fcgi?cmd=Retrieve&db=PubMed&dopt=Citation&list_uids=8876249

Road, P. (2009). Markov models for ion channels : versatility versus identifiability and speed. 2161–2179. doi: 10.1098/rsta.2008.0301

Roth, A., and Häusser, M. (2001). Compartmental models of rat cerebellar Purkinje cells based on simultaneous somatic and dendritic patch-clamp recordings. *Journal of physiology* 535, 445–472.

Roux, B., Allen, T., Berneche, S., and Im, W. (2004). Theoretical and computational models of biological ion channels. *Q Rev Biophys* 37, 15–103. Available at: http://www.ncbi.nlm.nih.gov/entrez/query.fcgi?cmd=Retrieve&db=PubMed&dopt=Citation&list_uids=17390604

Sakmann, B., and Neher, E. (1995). *Single-Channel Recording*., eds. B. Sakmann and E. Neher. New york and London: Plenum Press.

Saltelli, A., Ratto, M., Andres, T., Campolongo, F., Cariboni, J., Gatelli, D., et al. (2008). *Global sensitivity analysis: The primer*. John Wiley & Sons. doi: 10.1002/9780470725184

Schoen, A., Salehiomran, A., Larkum, M. E., and Cook, E. P. (2012). A Compartmental Model of Linear Resonance and Signal Transfer in Dendrites. *Neural Comput* 3144, 1–19. doi: 10.1162/NECO_a_00366

Segev, I., and Rall, W. (1998). Excitable dendrites and spines: earlier theoretical insights elucidate recent direct observations. *Trends Neurosci* 21, 453–460. Available at: http://www.ncbi.nlm.nih.gov/entrez/query.fcgi?cmd=Retrieve&db=PubMed&dopt=Citation&list_uids=9829684

Segev, I., and Schneidman, E. (1999). Axons as computing devices: basic insights gained from models. *J Physiol Paris* 93, 263–270. Available at: http://www.ncbi.nlm.nih.gov/entrez/query.fcgi?cmd=Retrieve&db=PubMed&dopt=Citation&list_uids=10574116

Sigg, D. (2014). Modeling ion channels: Past, present, and future. *J Gen Physiol* 144, 7–26. doi: 10.1085/jgp.201311130

Silver, R. A. (2010). Neuronal arithmetic. *Nat Rev Neurosci* 11, 474–489. doi: 10.1038/nrn2864

Sobol, I. M. (2001). Global sensitivity indices for nonlinear mathematical models and their Monte Carlo estimates. *Math Comput Simul* 55. doi: 10.1016/S0378-4754(00)00270-6

Spruston, N., and Kath, W. L. (2004). Dendritic arithmetic. *Nat Neurosci* 7, 567–569. Available at: http://www.ncbi.nlm.nih.gov/entrez/query.fcgi?cmd=Retrieve&db=PubMed&dopt=Citation&list_uids=15162161

Stuart, G. J., and Spruston, N. (2015). Dendritic integration: 60 years of progress. *Nat Neurosci* 18, 1713–1721. doi: 10.1038/nn.4157

Toledo-Rodriguez, M. P. M., Monier, C., Piwkowska, Z., Bal, T., Frégnac, Y., Markram, H., et al. (2008). Minimal Hodgkin – Huxley type models for different classes of cortical and thalamic neurons. *Biol Cybern* 99, 427–441. doi: 10.1007/s00422-008-0263-8

Wood, R., Gurney, K. N., and Wilson, C. J. (2004). A novel parameter optimisation technique for compartmental models applied to a model of a striatal medium spiny neuron. 60, 1109–1116. doi: 10.1016/j.neucom.2004.01.174

Yuste, R., and Church, G. M. (2014). The new century of the brain. *Sci Am* 310. doi: 10.1038/scientificamerican0314-38

Zi, Z. (2011). Sensitivity analysis approaches applied to systems biology models. *IET Syst Biol* 5. doi: 10.1049/iet-syb.2011.0015

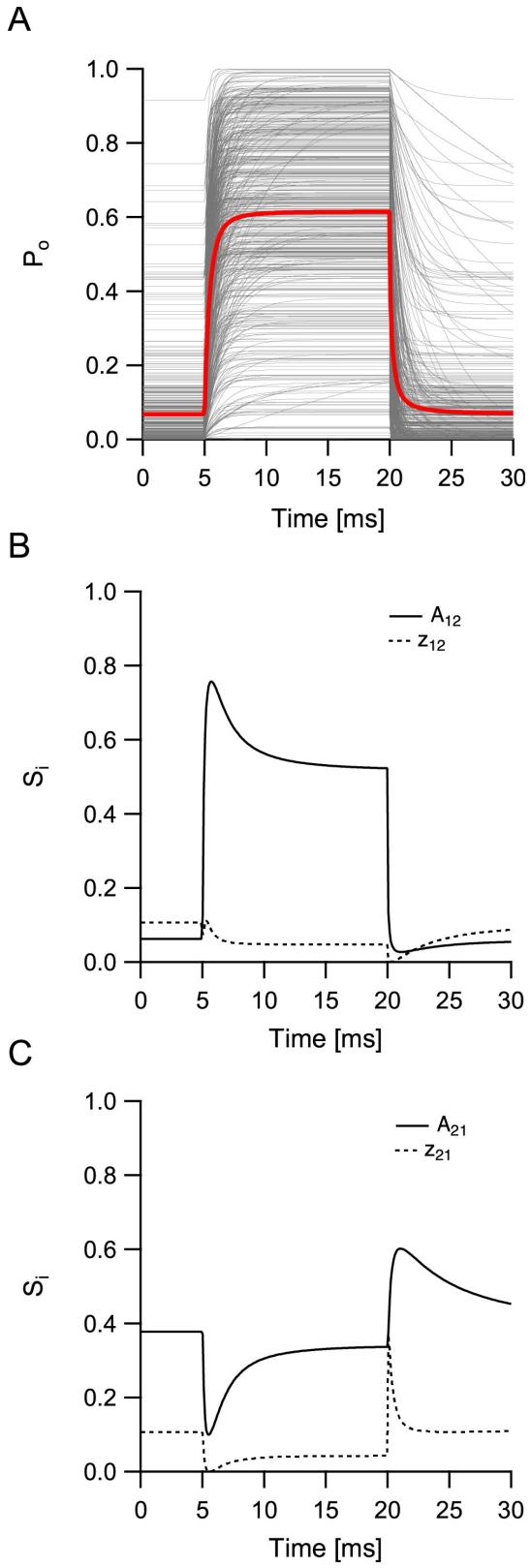
A
1.0
0.8
0.6
0.4
0.2
0.0
P_o
0
5
10
15
20
25
30
Time [ms]
B
1.0
0.8
0.6
0.4
0.2
0.0
S_i
A_{12}
z_{12}
0
5
10
15
20
25
30
Time [ms]
C
1.0
0.8
0.6
0.4
0.2
0.0
S_i
A_{21}
z_{21}
0
5
10
15
20
25
30
Time [ms]

Figure 1

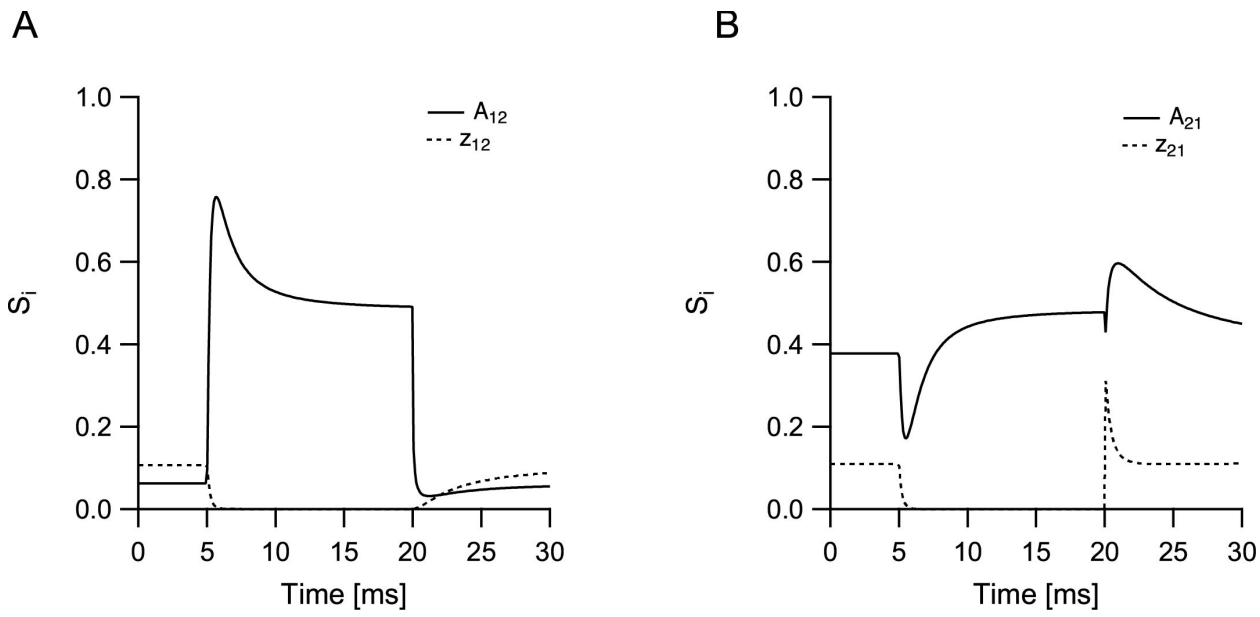

Figure 2

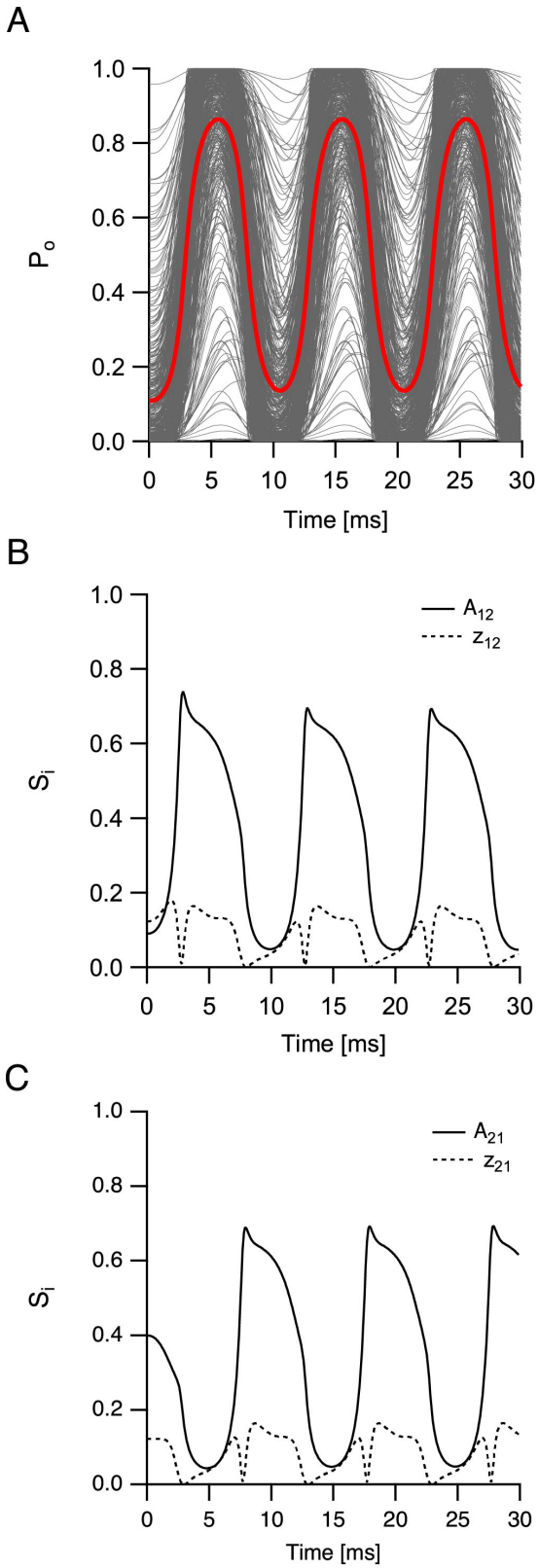
A
1.0
0.8
0.6
0.4
0.2
0.0
P_o
0
5
10
15
20
25
30
Time [ms]
B
1.0
0.8
0.6
0.4
0.2
0.0
S_i
A_{12}
z_{12}
0
5
10
15
20
25
30
Time [ms]
C
1.0
0.8
0.6
0.4
0.2
0.0
S_i
A_{21}
z_{21}
0
5
10
15
20
25
30
Time [ms]

Figure 3

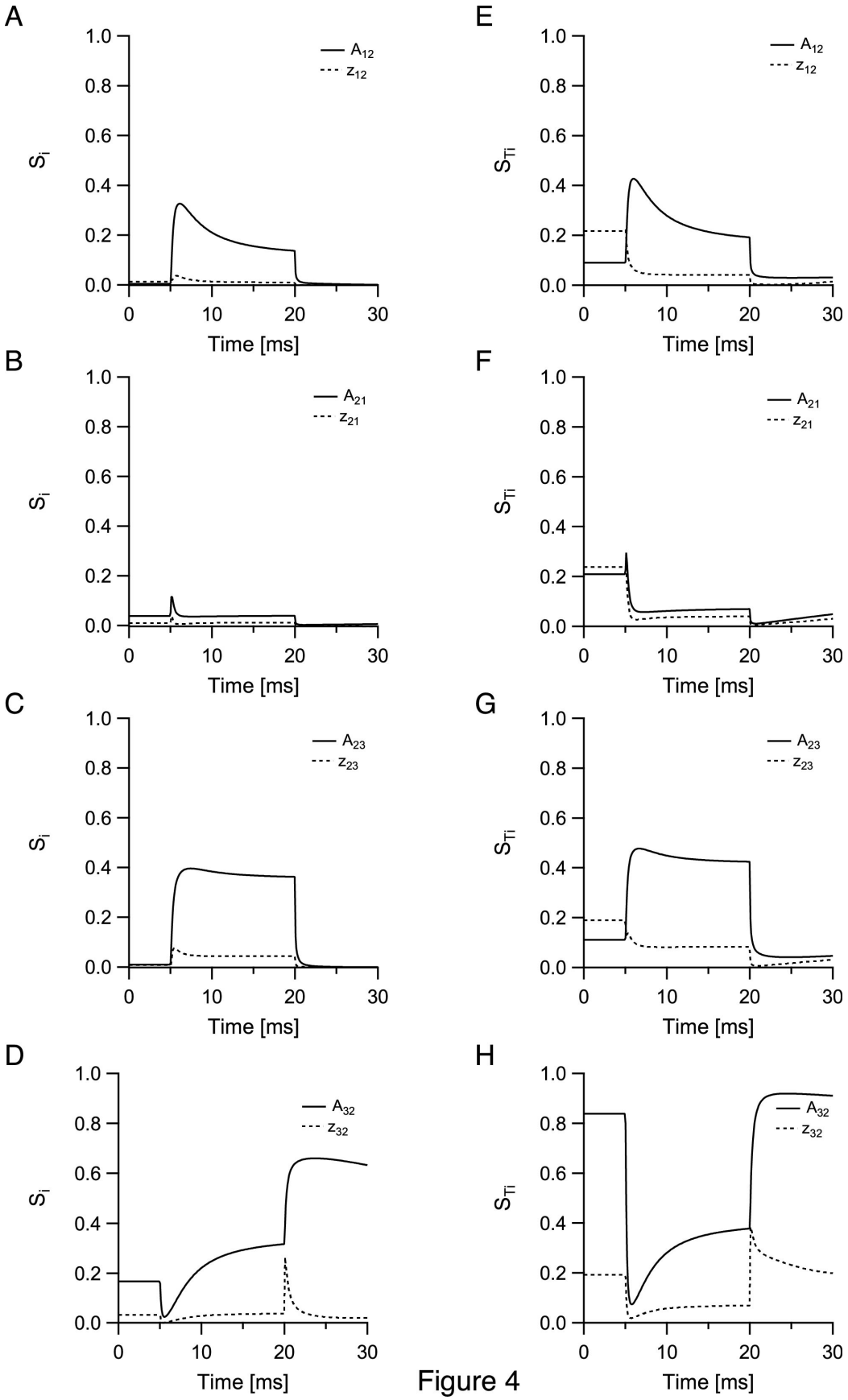

Figure 4

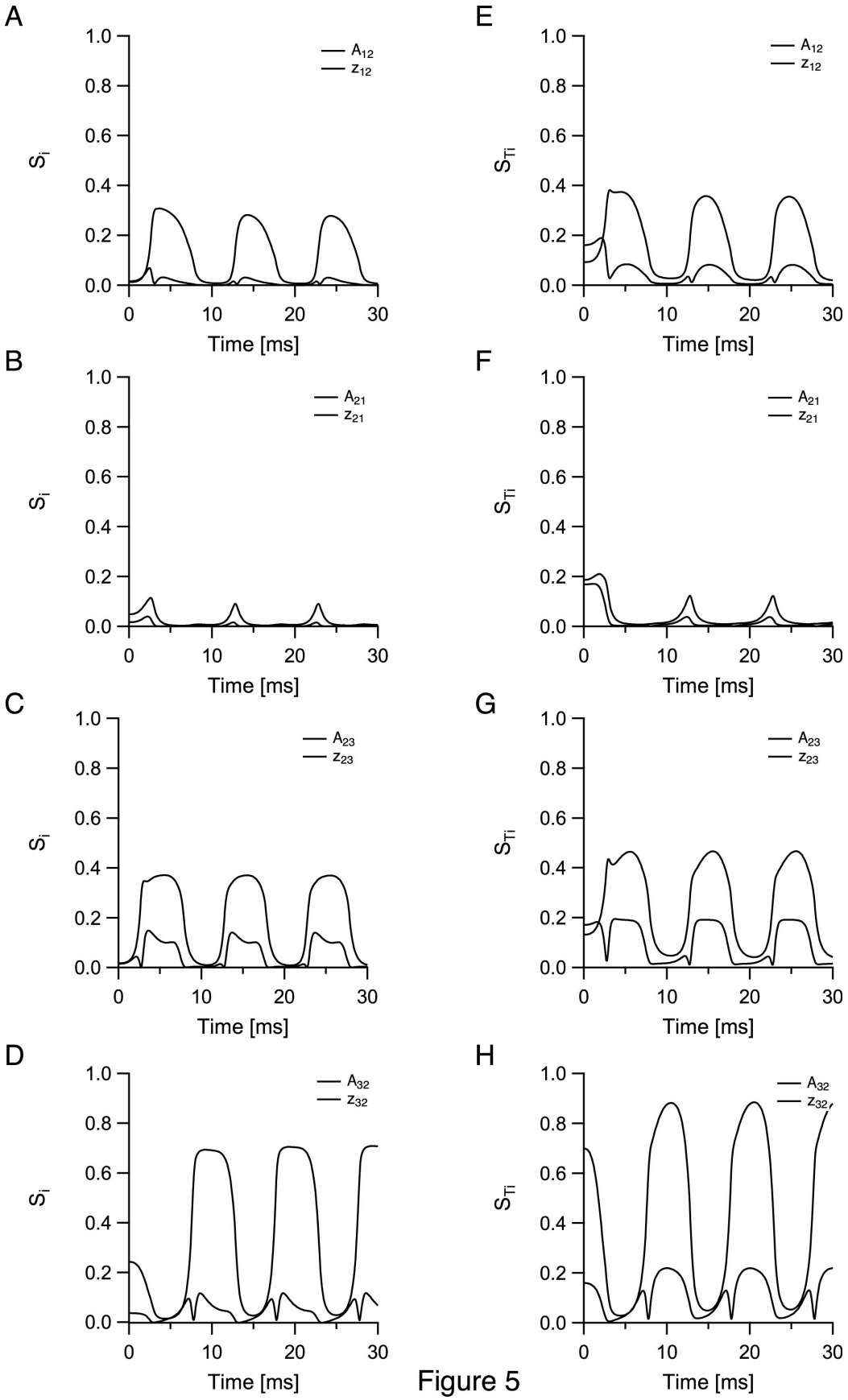

Figure 5

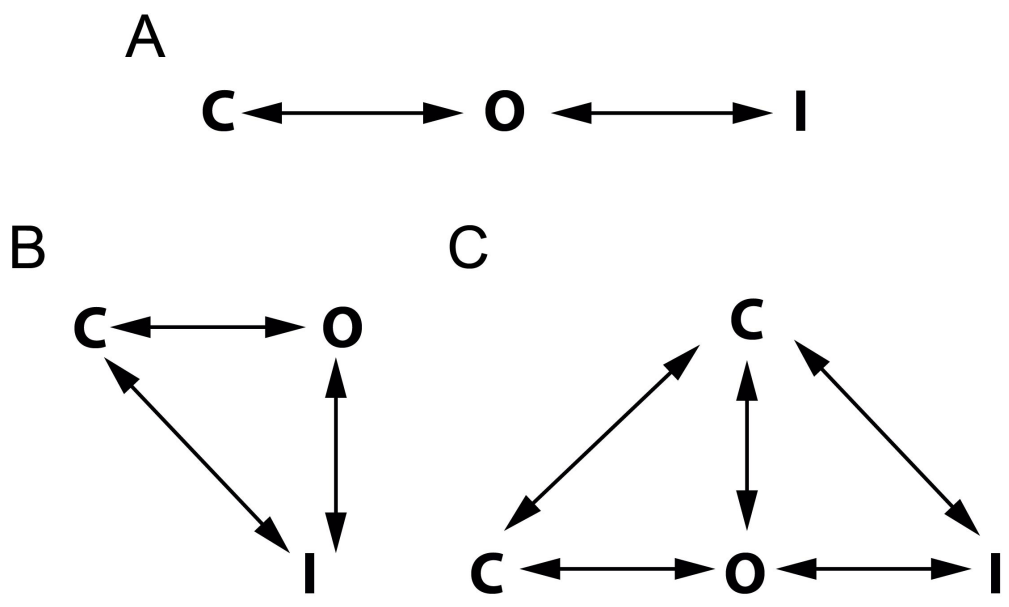

Figure 6